

DOI: 10.18721/JPM.10411

UDC 539.125

## **$N = 28$ ISOTONES: SHAPE COEXISTENCE TOWARDS PROTON DEFICIENT SIDE**

**G. Saxena<sup>1</sup>, M. Kaushik<sup>2</sup>**

<sup>1</sup>Government Women Engineering College, Ajmer, India;

<sup>2</sup>Shankara Institute of Technology, Jaipur, India

We have employed the RMF+BCS (relativistic mean-field plus BCS) approach to study the phenomenon of shape coexistence in  $N = 28$  isotones towards the proton-deficient side. Our present investigations include single particle energies, deformations, binding energies as well as excitation energies. It is found that towards the proton-deficient side,  $N = 28$  shell closure disappears due to reduced gap between neutron  $1f_{7/2}$  and  $1f_{5/2}$  and the nuclei  $^{40}\text{Mg}$ ,  $^{42}\text{Si}$ , and  $^{44}\text{S}$  are found to possess shape coexistence, giving further support to weakening of the shell gap. These results are found to be in excellent agreement with other theoretical and experimental studies and are fortified with a variety of calculations and parameters.

**Key words:** neutron magic nucleus; relativistic mean-field plus BCS approach; shape coexistence; shell closure

**Citation:** G. Saxena, M. Kaushik, M. Kumar,  $N = 28$  isotones: shape coexistence towards proton deficient side, St. Petersburg Polytechnical State University Journal. Physics and Mathematics. 10 (4) (2017) 134–142. DOI: 10.18721/JPM.10411

## **СОСУЩЕСТВОВАНИЕ ФОРМ ЯДЕР ИЗОТОНОВ, ИМЕЮЩИХ 28 НЕЙТРОНОВ И ДЕФИЦИТ ПРОТОНОВ**

**Г. Саксена<sup>1</sup>, М. Каушик<sup>2</sup>**

<sup>1</sup>Правительственный женский инженерный колледж, г. Аджмер, Индия;

<sup>2</sup>Технологический институт Шанкары, г. Джайпур, Индия

В работе теоретически изучено явление сосуществования форм ядер изотонов (нуклиды, имеющие одинаковое количество нейтронов в ядре,  $N = 28$  в данном случае, но разное количество протонов) при условии протонного дефицита. В расчетах использовано приближение RMF + BCS (релятивистская модель среднего поля плюс теория Бардина – Купера – Шриффера (БКШ)). Рассмотрены энергии одиночных частиц, деформации, энергетика связей, а также энергии возбуждения. Установлено, что заполнение энергетической оболочки ядра, состоящей из 28 нейтронов, нарушается ввиду протонного дефицита, вследствие уменьшения энергетической разности между нейтронными состояниями  $1f_{7/2}$  и  $1f_{5/2}$ . Также установлено, что ядра  $^{40}\text{Mg}$ ,  $^{42}\text{Si}$  и  $^{44}\text{S}$  обладают сосуществованием форм, приводящим к дальнейшему уменьшению указанной энергетической разности в оболочке ядра. Установлено, что полученные результаты находятся в прекрасном соответствии с данными других теоретических и экспериментальных исследований и подкреплены рядом расчетов и соответствующими значениями параметров.

**Ключевые слова:** магическое ядро; релятивистская модель среднего поля плюс теория БКШ; сосуществование форм; заполнение оболочки

**Ссылка при цитировании:** Саксена Г., Каушик М. Сосуществование форм ядер изотонов, имеющих 28 нейтронов и дефицит протонов // Научно-технические ведомости СПбГПУ. Физико-математические науки. 2017. Т. 10. № 4. С. 134–142. DOI: 10.18721/JPM.10411

## 1. Introduction

The evolution of ground-state shapes in an isotopic or an isotonic chain is governed by changes of the shell structure of a single-nucleon orbital. In recent past, evolution of shell structure guiding shape coexistence has been observed in the  $N = 20$  and  $N = 28$  isotones around the proton drip-line [1 – 4]. In a more general manner, the major structural features along the isotonic and isotopic chains around the spherical magic numbers 8, 20, 28, 50, 82, and 126 were reviewed by Sorlin et al. [5] using evolution of the binding energies, trends of first collective states and characterization of single-particle states. A number of experimental investigations have shown [3, 6] that in the proton-deficient  $N = 28$  isotones below  $^{48}\text{Ca}$  the spherical shell gap progressively reduces and the low-energy spectra of  $^{46}\text{Ar}$ ,  $^{44}\text{S}$ , and  $^{42}\text{Si}$  display evidence of ground-state deformation and shape coexistence.

Theoretical treatment of evolution of shell closure has been successfully described using mean-field theories [7 – 9] and with their relativistic counterparts [10 – 15]. The main advantage of the RMF + BCS (Relativistic Mean-Field plus Bardeen – Cooper – Schrieffer theory) approach is that it provides the spin-orbit interaction in the entire mass region in a natural way [10 – 12]. This indeed has proved to be very crucial for the study of nuclei near the drip-line. As nuclei move away from stability and approach the drip-lines, the corresponding Fermi surface gets closer to zero energy at the continuum threshold. A significant number of the available single-particle states then form part of the continuum. Indeed, the RMF + BCS scheme [11, 14] yields results which are in close agreement with the experimental data and with those of continuum relativistic Hartree – Bogoliubov (RCHB) and other similar mean-field calculations [15]. Recently, deformed relativistic Hartree – Bogoliubov (RHB) theory in continuum has been developed aiming at a proper description of exotic nuclei, particularly for  $^{42}\text{Mg}$  [16]. Moreover, development of the covariant density functional theory in continuum has been introduced for the description of neutron halo phenomena in medium heavy and heavy nuclei,

including the relativistic continuum Hartree – Bogoliubov theory, the relativistic Hartree – Fock – Bogoliubov theory in continuum and the deformed relativistic Hartree – Bogoliubov theory in continuum [17].

In recent past, the RMF approach has successfully investigated two-proton radioactivity [18], weakly bound drip-line nuclei [19] and magicity [20]. More recently, relativistic mean field study has extensively used to describe actinides and superheavy nuclei within covariant density functional theory [21], to calculate decay rates of various proton emitters [22], to study bubble structure [23], to analyze effects of particle-number fluctuation degree of freedom on symmetric and asymmetric spontaneous fission [24] and to calculate neutron capture cross-sections in nuclei near the  $N = 82$  shell closure [25].

In this paper, we have investigated the shape coexistence phenomenon for proton deficient  $N = 28$  isotones using the relativistic mean-field (RMF) plus BCS approach [18 – 20].

## 2. Relativistic mean-field model

Our RMF calculations have been carried out using the Lagrangian density model with nonlinear terms both for the  $\sigma$  and  $\omega$  mesons along with the TMA parametrization as described in detail in Refs. [12, 14, 18]:

$$\begin{aligned} \mathcal{L} = & \bar{\psi}[\gamma^\mu \partial_\mu - M]\psi + \frac{1}{2} \partial_\mu \sigma \partial^\mu \sigma - \frac{1}{2} m_\sigma^2 \sigma^2 - \\ & - \frac{1}{3} g_2 \sigma^3 - \frac{1}{4} g_3 \sigma^4 - g_\sigma \bar{\psi} \sigma \psi - \frac{1}{4} H_{\mu\nu} H^{\mu\nu} + \\ & + \frac{1}{2} m_\omega^2 \omega_\mu \omega^\mu + \frac{1}{4} c_3 (\omega_\mu \omega^\mu)^2 - g_\omega \bar{\psi} \gamma^\mu \psi \omega_\mu - \\ & - \frac{1}{4} G_{\mu\nu}^a G^{a\mu\nu} + \frac{1}{2} m_\rho^2 \rho_\mu^a \rho^{a\mu} - \frac{1}{4} H_{\mu\nu} H^{\mu\nu} - \\ & - e \bar{\psi} \gamma_\mu \frac{(1 - \tau_3)}{2} A^\mu \psi, \end{aligned} \quad (1)$$

where the field tensors  $H$ ,  $G$  and  $F$  for the vector fields are defined by

$$\begin{aligned} H_{\mu\nu} &= \partial_\mu \omega_\nu - \partial_\nu \omega_\mu, \\ G_{\mu\nu}^a &= \partial_\mu \rho_\nu^a - \partial_\nu \rho_\mu^a - 2g_\rho \epsilon^{abc} \rho_\mu^b \rho_\nu^c, \\ F_{\mu\nu} &= \partial_\mu A_\nu - \partial_\nu A_\mu, \end{aligned}$$

and other symbols have their usual meaning.

Based on the single-particle spectrum calculated by the RMF described above, we perform state dependent BCS calculations [26, 27]. The continuum is replaced by a set of positive energy states generated by enclosing the nucleus in a spherical box. Thus, the gap equations have the standard form for all the single particle states, i.e.,

$$\Delta_{j_1} = -\frac{1}{2} \frac{1}{\sqrt{2j_1 + 1}} \times \sum_{j_2} \frac{\langle (j_1^2)0^+ |V| (j_2^2)0^+ \rangle}{\sqrt{(\varepsilon_{j_2} - \lambda)^2 + \Delta_{j_2}^2}} \sqrt{2j_2 + 1} \Delta_{j_2}, \quad (2)$$

where  $\varepsilon_{j_2}$  are the single particle energies, and  $\lambda$  is the Fermi energy, whereas the particle number condition is given by

$$\sum_j (2j + 1)v_j^2 = N.$$

In the calculations we use for the pairing interaction a delta-force, i.e.,  $V = -V_0\delta(r)$  with the same strength  $V_0 = 350 \text{ MeV}/(\text{fm})^3$  for both protons and neutrons [14].

Apart from its simplicity, the applicability and justification of using such a  $\delta$ -function form of interaction was discussed in Ref. [28], where it was shown in the context of HFB calculations that the use of a delta-force in a finite space simulates the effect of finite range interaction in a phenomenological manner. The pairing matrix element for the  $\delta$ -function force is given by

$$\begin{aligned} & \langle (j_1^2)0^+ |V| (j_2^2)0^+ \rangle = \\ & = -\frac{V_0}{8\pi} \sqrt{(2j_1 + 1)(2j_2 + 1)} I_R, \end{aligned} \quad (3)$$

where  $I_R$  is the radial integral having the form

$$I_R = \int dr \frac{1}{r^2} (G_{j_1}^* G_{j_2} + F_{j_1}^* F_{j_2})^2. \quad (4)$$

Here  $G_\alpha$  and  $F_\alpha$  denote the radial wave functions for the upper and lower components, respectively, of the nucleon wave function expressed as

$$\Psi_\alpha = \frac{1}{r} \begin{pmatrix} iG_\alpha Y_{j_\alpha l_\alpha m_\alpha} \\ F_\alpha \sigma \cdot \hat{r} Y_{j_\alpha l_\alpha m_\alpha} \end{pmatrix}, \quad (5)$$

and satisfy the normalization condition

$$\int dr \{|G_\alpha|^2 + |F_\alpha|^2\} = 1. \quad (6)$$

In Eq. (5) the symbol  $Y_{jlm}$  is used for the standard spinor spherical harmonics with the phase  $i^l$ . The coupled field equations obtained from the Lagrangian density in Eq. (1) are finally reduced to a set of simple radial equations which are solved self-consistently along with the equations for the state dependent pairing gap  $\Delta_j$  and the total particle number  $N$  for a given nucleus.

The relativistic mean field description was extended for the deformed nuclei of axially symmetric shapes by Gambhir, Ring and their collaborators [11] using an expansion method. The treatment of pairing was carried out in Ref. [29] using state dependent BCS method as given in Ref. [18] for the spherical case. For axially deformed nuclei the rotational symmetry is no more valid and the total angular momentum  $j$  is no longer a good quantum number. Nevertheless, the various densities still are invariant with respect to a rotation around the symmetry axis. Here we took the symmetry axis to be the  $z$ -axis. Following Gambhir et al. [11], it was then convenient to employ the cylindrical coordinates

$$x = r_\perp \cos\varphi, \quad y = r_\perp \sin\varphi \quad \text{and} \quad z. \quad (7)$$

The spinor  $\psi_i$  with the index  $i$  is now labeled by the quantum numbers  $\Omega_i$ ,  $\pi_i$  and  $t_i$ , where  $\Omega_i$  is the eigenvalue of the symmetry operator  $j_z$  (the projection of  $j_i$  on the  $z$ -axis),  $\pi_i$  indicates the parity and  $t_i$  has been used for the isospin.

In terms of these quantum numbers, the spinor can now be expressed in the following form:

$$\begin{aligned} \psi_i(\mathbf{r}, t) &= \begin{pmatrix} f_i(\mathbf{r}) \\ ig_i(\mathbf{r}) \end{pmatrix} = \\ &= \frac{1}{\sqrt{2\pi}} \begin{pmatrix} f_i^+(z, r_\perp) e^{i(\Omega_i - 1/2)\varphi} \\ f_i^-(z, r_\perp) e^{i(\Omega_i + 1/2)\varphi} \\ ig_i^+(z, r_\perp) e^{i(\Omega_i - 1/2)\varphi} \\ ig_i^-(z, r_\perp) e^{i(\Omega_i + 1/2)\varphi} \end{pmatrix} \chi_{t_i}(t). \end{aligned} \quad (8)$$

Here the four components  $f_i(r_\perp, z)$  and  $g_i(r_\perp, z)$  obey the Dirac equations.

For the axially symmetric case the spinors

$f_i(r_\perp, z)$  and  $g_i(r_\perp, z)$  are expanded in terms of the eigenfunctions of a deformed axially symmetric oscillator potential as described in Refs. [11, 29]. The pairing gap  $\Delta_k$  satisfies the gap equation

$$\Delta_k = \frac{1}{2} \sum_{k' > 0} \frac{\bar{V}_{kk'} |\Delta_{k'}|}{\sqrt{(\varepsilon_{k'} - \lambda)^2 + \Delta_{k'}^2}}. \quad (9)$$

Here the symbols  $\varepsilon_{k'}$  and  $\lambda$  denote the single particle and Fermi energy, whereas the pairing matrix element  $V_{kk'}$  for the symmetrically deformed case using the zero-range  $\delta$ -force is given by

$$\begin{aligned} \bar{V}_{ij} &= \langle \bar{ii} | V | \bar{jj} \rangle - \langle \bar{ii} | V | \bar{jj} \rangle = \quad (10) \\ &= -V_0 \int d^3r [\psi_i^\dagger \psi_i^\dagger \psi_j^\dagger \psi_j^\dagger - \psi_i^\dagger \psi_i^\dagger \psi_j^\dagger \psi_j^\dagger]. \quad (11) \end{aligned}$$

For further details of these formulations we refer the reader to Refs. [11, 18, 29]. In addition, to get a more detailed picture of deformation in various other theories readers may refer to deformed relativistic Hartree – Bogoliubov (RHB) theory in continuum [16], deformed relativistic Hartree – Bogoliubov (DRHB) theory [30] and multidimensionally-constrained relativistic mean field (MDC-RMF) theory [31, 32].

### 3. Results and discussion

The binding energy maps exhibit variety of rapidly evolving shapes after successive removals of proton pairs towards the drip-line of  $N = 28$  isotones. This variation of binding energy is shown in Fig. 1 with respect to the quadrupole deformation parameter  $\beta_{2m}$  for  $N = 28$  isotones. As established and expected, we found a spherical configuration of doubly-magic  $^{48}\text{Ca}$  with one sharp minimum at  $\beta_{2m} = 0$ . Towards the proton-rich side we have also found a spherical configuration for  $^{50}\text{Ti}$  (see Fig. 1). By removing a pair of protons from  $^{48}\text{Ca}$ , the energy surface of the corresponding isotone  $^{46}\text{Ar}$  becomes soft with a shallow extended minimum along the oblate axis (shown in upper right panel). After another removal of a proton pair we obtained a coexistence of prolate and oblate minima at  $\beta_{2m} = 0.38$  and  $-0.26$  respectively for the nucleus  $^{44}\text{S}$  as can be observed from the upper left panel of Fig. 1. These two minima are separated only by an excitation energy of 0.77 MeV and, therefore, we can expect to find pronounced mixing of prolate and oblate configurations in the low-energy collective states of this nucleus. Next, for  $^{42}\text{Si}$  the binding energy displays a deep oblate minimum at  $\beta_{2m} = -0.37$  whereas the

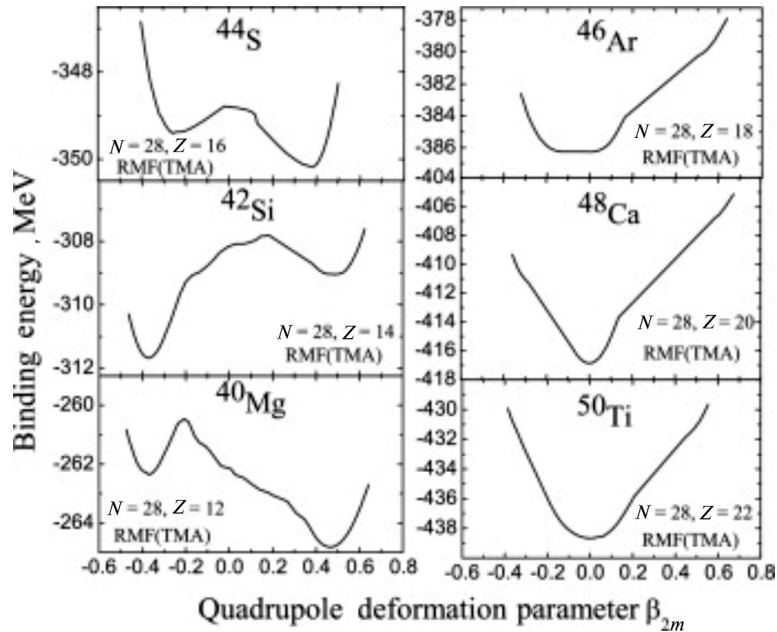


Fig. 1. The potential energy surface of  $N = 28$  isotones (6 nuclei) as a function of the deformation parameter  $\beta_{2m}$

Table 1

Calculation results of excitation energy values compared to those of other authors

Nucleus	Excitation energy, MeV	
	Our study	Other data
<sup>44</sup> S	0.77	1.36 [33], 0.2 [1]
<sup>42</sup> Si	2.60	2.50 [34], 1.5 [1]
<sup>40</sup> Mg	3.50	1.38 [35]

Notes. The excitation energy is an energy difference between two minima as obtained in the deformed RMF calculations using TMA force parameters. Our results are compared with both theoretical and experimental ones [1, 33 – 35].

second prolate minimum is found at  $\beta_{2m} = 0.49$  with an excitation energy of 2.6 MeV (see Fig. 1, the middle left panel). These results are similar to those obtained from the RHB theory by Lalazissis et al. [1] and the energy density functional analysis of shape evolution in  $N = 28$  isotones [4]. Furthermore, with another proton pair removed, the very neutron-rich nucleus <sup>40</sup>Mg shows a deep prolate minimum at  $\beta_{2m} = 0.46$  and an oblate minimum at  $\beta_{2m} = -0.37$  with the excitation energy of 3.5 MeV (see Fig. 1, lower left panel).

One important observation that can be made from Fig. 1 is that successive removal of protons leads to complete change in the shapes. As can be seen from Fig. 1, <sup>44</sup>S has a more likely prolate shape due to the prolate minima standing below the oblate minima. With two protons less in <sup>42</sup>Si, oblate minima occur below the prolate minima, resulting in <sup>42</sup>Si having a

more likely oblate shape, whereas again with two protons less in <sup>40</sup>Mg, the existence of a prolate shape becomes more pronounced.

Therefore, from the variation shown in Fig. 1 we can conclude that the phenomenon of shape coexistence indeed exists towards the proton-deficient nuclei of  $N = 28$  isotones. We found the excitation energy (energy difference between two minima) for the nuclei <sup>40</sup>Mg, <sup>42</sup>Si, <sup>44</sup>S due to shape mixing (Table 1), which are also compared with some other theoretical and experimental data [1, 33–35]. It is gratifying to note that our results are in good agreement with other data which confirm the shape coexistence in  $N = 28$  isotone towards the proton-deficient side.

To compare our results with other theoretical calculations and experiments, in Table 2, we have shown quadrupole deformation for neutron-rich  $N = 28$  isotones.

Table 2

Results of quadrupole deformation parameter for  $N = 28$  isotones

Nucleus	Quadrupole deformation parameter			
	RMF (TMA)	Experiment [36]	FRDM [37]	HFB [38]
<sup>40</sup> Mg	0.477	–	0.312	0.36
<sup>42</sup> Si	–0.375	–	0.393	–0.33
<sup>44</sup> S	0.380	0.254	0.247	–0.27
<sup>46</sup> Ar	0.000	0.175	0.135	–0.20
<sup>48</sup> Ca	0.000	0.106	0.000	0.12

Note: RMF(TMA) results are obtained in this study.

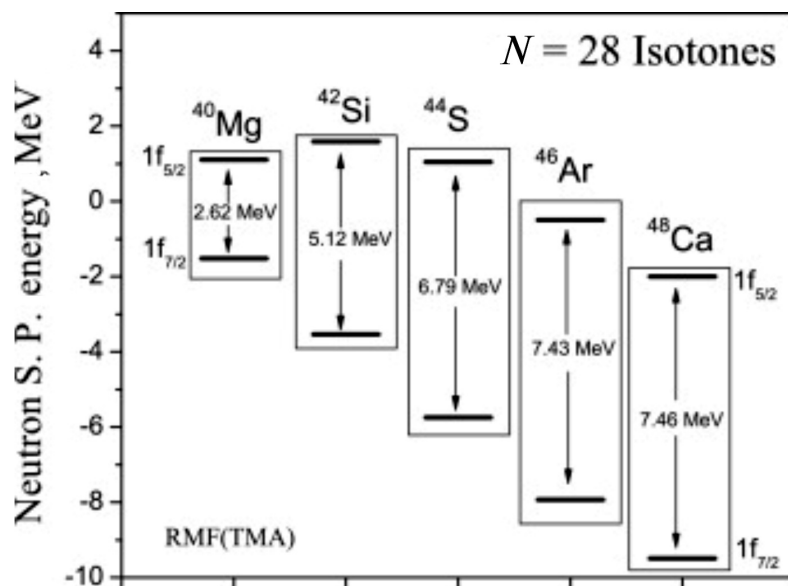


Fig. 2. Calculation results of energy difference between neutron  $1f_{5/2}$  and  $1f_{7/2}$  states responsible for  $N = 28$  shell closure for five nuclei

As shown in the case of  $^{48}\text{Ca}$ , magic nuclei possess a spherical configuration and therefore phenomenon of shape coexistence results to disappearance of  $N = 28$  neutron shell closure. To demonstrate it we show in Fig. 2 the energy difference between neutron  $1f_{5/2}$  and  $1f_{7/2}$  states which gives rise to  $N = 28$  shell closure. These single particle energies are calculated using the RMF framework with a spherical configuration [14, 20]. It is evident from Fig. 2 that the gap decreases significantly towards proton deficient side from 7.49 MeV for  $^{48}\text{Ca}$  to 2.62 MeV for  $^{40}\text{Mg}$ . This drastic change for the proton-deficient nuclei gives rise to the disappearance of  $N = 28$  shell closure and the development of the phenomenon of shape coexistence.

#### 4. Summary

In this paper, we have investigated the shape coexistence phenomenon in  $N = 28$  isotones by employing relativistic mean-field plus BCS (RMF+BCS) approach [18 – 20]. For our study, the RMF calculations were carried out using the TMA parameter, and the results of single particle spectra, binding energy, excitation energy, etc., were analyzed for the phenomenon of the shape coexistence. We found through variation of binding energy with

quadrupole deformation that  $N = 28$  isotones indeed showed shape coexistence towards the proton drip-line. Neutron-rich  $^{40}\text{Mg}$ ,  $^{42}\text{Si}$ , and  $^{44}\text{S}$  were found with mixed configuration of prolate and oblate shapes. This shape mixing in  $N = 28$  isotones results in the collapse of spherical configuration and consequently  $N = 28$  shell closure. It is indulging to note that our results of excitation energy are in good match with other communications [1, 33 – 35]. In addition to this, we also focused on single particle energies of  $1f_{5/2}$  and  $1f_{7/2}$  states and it was found that this shell gap decreased towards the proton-deficient side fortifying the conclusion of disappearance of  $N = 28$  shell closure and shape coexistence.

#### Acknowledgements

Authors would like to thank Prof. H.L. Yadav, Banaras Hindu University, Varanasi, India, for his kind guidance and continuous support. The authors are indebted to Dr. L.S. Geng, RCNP, Osaka, Japan, for valuable correspondence. One of the authors (G. Saxena) gratefully acknowledges the support provided by Science and Engineering Research Board (DST), Government of India, under the young scientist project YSS/2015/000952.

## REFERENCES

- [1] **G.A. Lalazissis, D. Vretenar, P. Ring, M. Stoitsov, L. Robledo**, Relativistic Hartree–Bogolyubov description of the deformed  $N = 28$  region, *Phys. Rev. C.* 60 (1) (1999) 014310.
- [2] **D. Vretenar, P. Ring, G.A. Lalazissis**, Relativistic mean field description of nuclei at the drip lines, *AIP Conf. Proc.* 481 (1) (1999) 91–104.
- [3] **C. Force, S. Grévy, L. Gaudefroy, O. Sorlin, L. Caceres, F. Rotaru, J. Mrazek**, Prolate-spherical shape coexistence at  $N = 28$  in  $^{44}\text{S}$ , *Phys. Rev. Lett.* 105 (10) (2010) 102501.
- [4] **Z.P. Li, J.M. Yao, D. Vretenar, T. Niki, H. Chen, J. Meng**, Energy density functional analysis of shape evolution in  $N = 28$  isotones, *Phys. Rev. C.* 84 (5) (2011) 054304.
- [5] **O. Sorlin, M.G. Porquet**, Nuclear magic numbers: new features far from stability, *Prog. Part. Nucl. Phys.* 61 (2) (2008) 602–673.
- [6] **L. Gaudefroy, J.M. Daugas, M. Hass, et al.**, Shell erosion and shape coexistence in  $^{43}\text{S}_{27}$ , *Phys. Rev. Lett.* 102 (9) (2009) 092501.
- [7] **K. Bennaceur, J. Dobaczewski, M. Ploszajczak**, Pairing anti-halo effect, *Phys. Lett. B.* 496 (3) (2000) 154–160.
- [8] **M. Grasso, N. Sandulescu, Nguyen Van Giai, R.J. Liotta**, Pairing and continuum effects in nuclei close to the drip line, *Phys. Rev. C.* 64 (6) (2001) 064321.
- [9] **N. Sandulescu, Nguyen Van Giai, R.J. Liotta**, Resonant continuum in the Hartree – Fock + BCS approximation, *Phys. Rev. C.* 61 (6) (2000) 061301(R).
- [10] **P.G. Reinhard**, The relativistic mean-field description of nuclei and nuclear dynamics, *Rep. Prog. Phys.* 52 (4) (1989) 439.
- [11] **Y.K. Gambhir, P. Ring, A. Thimet**, Relativistic mean-field theory for finite nuclei, *Ann. Phys.* 198 (1) (1990) 132–179.
- [12] **Y. Sugahara, H. Toki**, Relativistic mean-field theory for unstable nuclei with nonlinear  $\sigma$  and  $\omega$  terms, *Nucl. Phys. A.* 579 (3–4) (1994) 557–572.
- [13] **P. Ring**, Relativistic mean-field theory in finite nuclei, *Prog. Part. Nucl. Phys.* 37 (1996) 193–263.
- [14] **H.L. Yadav, S. Sugimoto, H. Toki**, Relativistic mean field plus BCS approach to drip-line nuclei, *Mod. Phys. Lett. A.* 17 (38) (2002) 2523–2533.
- [15] **J. Meng, H. Toki, S.G. Zhou, S.Q. Zhang, W.H. Long, L.S. Geng**, Relativistic continuum Hartree–Bogoliubov theory for ground state properties of exotic nuclei, *Prog. Part. Nucl. Phys.* 57 (2) (2006) 470–563.
- [16] **L. Li, J. Meng, P. Ring, E.G. Zhao, S.G. Zhou**, Deformed relativistic Hartree–Bogoliubov theory in continuum, *Phys. Rev. C.* 85 (2) (2012) 024312.
- [17] **J. Meng, S.G. Zhou**, Halos in medium-heavy and heavy nuclei with covariant density functional theory in continuum, *J. Phys. G.* 42 (9) (2015) 093101.
- [18] **D. Singh, G. Saxena, M. Kaushik, H.L. Yadav, H. Toki**, Study of two-proton radioactivity within relativistic mean-field plus BCS approach, *Int. Jour. of Mod. Phys. E.* 21 (9) (2012) 1250076.
- [19] **G. Saxena, D. Singh, M. Kaushik, S. Somorendro Singh**, RMF+BCS approach for drip-line isotopes of Si, *Canadian J. Phys.* 92 (3) (2014) 253–258.
- [20] **G. Saxena, D. Singh**, Shell closure, loosely bound structure and halos in exotic nuclei, *J. Exp. Theor. Phys.* 116 (4) (2013) 567–578.
- [21] **A.V. Afanasjev, S.E. Agbemava**, Nuclear structure theory of the heaviest nuclei, *Acta Phys. Polon. B.* 46 (3) (2015) 405–417.
- [22] **Y. Qian, Z. Ren**, Calculations on decay rates of various proton emissions, *Eur. Phys. J. A.* 52 (3) (2016) 1–7.
- [23] **A. Shukla, S. Aberg, A. Bajpeyi**, Systematic study of bubble nuclei in relativistic mean field model, *Phys. Atom Nucl.* 79 (1) (2016) 11–20.
- [24] **J. Zhao**, Multidimensionally-constrained relativistic mean-field study of spontaneous fission: Coupling between shape and pairing degrees of freedom, *Phys. Rev. C.* 93 (4) (2016) 044315.
- [25] **S. Dutta, D. Chakraborty, G. Gangopadhyay, A. Bhattacharyya**, Neutron capture reactions near the  $N = 82$  shell-closure, *Phys. Rev. C.* 93 (2) (2016) 024602.
- [26] **A.M. Lane**, Nuclear theory: pairing force correlations and collective motion, Benjamin, New York, 1964.
- [27] **P. Ring, P. Schuck**, The nuclear many-body problem, Springer, Berlin, 1980.
- [28] **J. Dobaczewski, H. Flocard, J. Treiner**, Hartree–Fock–Bogolyubov description of nuclei near the neutron-drip line, *Nucl. Phys. A.* 422 (1) (1984) 103–139.
- [29] **L.S. Geng, H. Toki, S. Sugimoto, J. Meng**, Relativistic mean field theory for deformed nuclei with the pairing correlations, *Prog. Theor. Phys.* 110 (5) (2003) 921–936.
- [30] **S.G. Zhou, J. Meng, P. Ring, E.G. Zhao**, Neutron halo in deformed nuclei, *Phys. Rev. C.* 82 (1) (2010) 011301(R).
- [31] **B.N. Lu, J. Zhao, E.G. Zhao, S.G. Zhou**, Multidimensionally-constrained relativistic mean-field models and potential-energy surfaces of actinide nuclei, *Phys. Rev. C.* 89 (1) (2014) 014323.
- [32] **S.G. Zhou**, Multidimensionally constrained covariant density functional theories nuclear shapes and potential energy surfaces, *Physica Scripta.* 91 (6) (2016) 063008.
- [33] **S. Grévy, F. Negoita, I. Stefan**, Observation of the  $0_2^+$  state in  $^{44}\text{S}$ , *Eur. Phys. J. A.* 25 (1Supl)

(2005) 111–113.

[34] **J.A. Tostevin, B.A. Brown, E.C. Simpson**, Two-proton removal from  $^{44}\text{S}$  and the structure of  $^{42}\text{Si}$ , *Phys. Rev. C.* 87 (2) (2013) 027601–027604.

[35] **R. Rodriguez-Guzmán, J.L. Egido, L.M. Robledo**, Correlations beyond the mean field in magnesium isotopes: angular momentum projection and configuration mixing, *Nucl. Phys. A.* 709 (1–4) (2002) 201–235.

[36] **S. Raman, C.W. Nestor jr., P. Tikkanen**, Transition probability from the ground to the first

*Received 20.08.2016, accepted 09.10.2017.*

excited  $2^+$  state of even-even nuclides, *At. Data Nucl. Data Tables.* 78 (1) (2001) 1–128.

[37] **P. Möller, A.J. Sierk, T. Ichikawa, H. Sagawa**, Nuclear ground-state masses and deformations: FRDM (2012), *Atomic Data and Nuclear Data Tables.* 109–110 (2016) 1–204.

[38] **S. Goriely, N. Chamel, J.M. Pearson**, Skyrme–Hartree–Fock–Bogoliubov nuclear mass formulas: crossing the 0.6 MeV accuracy threshold with microscopically deduced pairing, *Phys. Rev. Lett.* 102 (15) (2009) 152503.

#### THE AUTHORS

##### SAXENA Gaurav

*Government Women Engineering College*

Makhapura, Nasirabad Road, Ajmer, Rajasthan 305002, India  
gauravphy@gmail.com

##### KAUSHIK Manish

*Shankara Institute of Technology*

RIICO Industrial Area (Delhi Jaipur Highway) Kukas, Jaipur, Rajasthan 302028, India

#### СПИСОК ЛИТЕРАТУРЫ

1. **Lalazissis G.A., Vretenar D., Ring P., Stoitsov M., Robledo L.** Relativistic Hartree–Bogolyubov description of the deformed  $N = 28$  region // *Phys. Rev. C.* 1999. Vol. 60. No. 1. P. 014310.

2. **Vretenar D., Ring P., Lalazissis G.A.** Relativistic mean-field description of nuclei at the drip lines // *AIP Conf. Proc.* 1999. Vol. 481. No. 1. Pp. 91–104.

3. **Force C., Grévy S., Gaudefroy L., Sorlin O., Caceres L., Rotaru F., Mrazek J.** Prolate-spherical shape coexistence at  $N = 28$  in  $^{44}\text{S}$ , *Phys. Rev. Lett.* 2010. Vol. 105. No. 10. P. 102501.

4. **Li Z.P., Yao J.M., Vretenar D., Niki T., Chen H., Meng J.** Energy density functional analysis of shape evolution in  $N = 28$  isotones // *Phys. Rev. C.* 2011. Vol. 84. No. 5. P. 054304.

5. **Sorlin O., Porquet M.G.** Nuclear magic numbers: new features far from stability // *Prog. Part. Nucl. Phys.* 2008. Vol. 61. No. 2. Pp. 602–673.

6. **Gaudefroy L., Daugas J.M., Hass M., et al.** Shell erosion and shape coexistence in  $^{43}\text{S}_{27}$ , *Phys. Rev. Lett.* 2009. Vol. 102. No. 9. P. 092501.

7. **Bennaceur K., Dobaczewski J., Ploszajczak M.** Pairing anti-halo effect // *Phys. Lett. B.* 2000. Vol. 496. No. 3. Pp. 154–160.

8. **Grasso M., Sandulescu N., Nguyen Van Giai, Liotta R.J.** Pairing and continuum effects in nuclei close to the drip line // *Phys. Rev. C.* 2001. Vol. 64. No. 6. P. 064321.

9. **Sandulescu N., Nguyen Van Giai, Liotta R.J.** Resonant continuum in the Hartree – Fock + BCS

approximation // *Phys. Rev. C.* 2000. Vol. 61. No. 6. P. 061301(R).

10. **Reinhard P.G.** The relativistic mean-field description of nuclei and nuclear dynamics // *Rep. Prog. Phys.* 1989. Vol. 52. No. 4. P. 439.

11. **Gambhir Y.K., Ring P., Thimet A.** Relativistic mean-field theory for finite nuclei // *Ann. Phys.* 1990. Vol. 198. No. 1. Pp. 132–179.

12. **Sugahara Y., Toki H.** Relativistic mean-field theory for unstable nuclei with nonlinear  $\sigma$  and  $\omega$  terms // *Nucl. Phys. A.* 1994. Vol. 579. No. 3–4. Pp. 557–572.

13. **Ring P.** Relativistic mean-field theory in finite nuclei // *Prog. Part. Nucl. Phys.* 1996. Vol. 37. Pp. 193–263.

14. **Yadav H.L., Sugimoto S., Toki H.** Relativistic mean-field plus BCS approach to drip-line nuclei // *Mod. Phys. Lett. A.* 2002. Vol. 17. No. 38. Pp. 2523–2533.

15. **Meng J., Toki H., Zhou S.G., Zhang S.Q., Long W.H., Geng L.S.** Relativistic continuum Hartree–Bogoliubov theory for ground state properties of exotic nuclei // *Prog. Part. Nucl. Phys.* 2006. Vol. 57. No. 2. Pp. 470–563.

16. **Li L., Meng J., Ring P., Zhao E.G., Zhou S.G.** Deformed relativistic Hartree–Bogoliubov theory in continuum // *Phys. Rev. C.* 2012. Vol. 85. No. 2. P. 024312.

17. **Meng J., Zhou S.G.** Halos in medium-heavy and heavy nuclei with covariant density functional theory in continuum // *J. Phys. G.* 2015. Vol. 42.



No. 9. P. 093101.

18. **Singh D., Saxena G., Kaushik M., Yadav H.L., Toki H.** Study of two-proton radioactivity within relativistic mean-field plus BCS approach // Int. J. of Mod. Phys. E. 2012. Vol. 21. No. 9. P. 1250076.

19. **Saxena G., Singh D., Kaushik M., Somorendro Singh S.** RMF+BCS approach for drip-line isotopes of Si // Canadian J. Phys. 2014. Vol. 92. No. 3. Pp. 253–258.

20. **Saxena G., Singh D.** Shell closure, loosely bound structure and halos in exotic nuclei // J. Exp. Theor. Phys. 2013. Vol. 116. No. 4. Pp. 567–578.

21. **Afnasjev A.V., Agbemava S.E.** Nuclear structure theory of the heaviest nuclei // Acta Phys. Polon. B. 2015. Vol. 46. No. 3. Pp. 405–417.

22. **Qian Y., Ren Z.** Calculations on decay rates of various proton emissions // Eur. Phys. J. A. 2016. Vol. 52. No. 3. Pp. 1–7.

23. **Shukla A., Aberg S., Bajpeyi A.** Systematic study of bubble nuclei in relativistic mean field model // Phys. Atom Nucl. 2016. Vol. 79. No. 1. Pp. 11–20.

24. **Zhao J.** Multidimensionally-constrained relativistic mean-field study of spontaneous fission: Coupling between shape and pairing degrees of freedom // Phys. Rev. C. 2016. Vol. 93. No. 4. P. 044315.

25. **Dutta S., Chakraborty D., Gangopadhyay G., Bhattacharyya A.** Neutron capture reactions near the  $N = 82$  shell-closure // Phys. Rev. C. 2016. Vol. 93. No. 2. P. 024602.

26. **Lane A.M.** Nuclear theory: pairing force correlations and collective motion. New York: Benjamin, 1964.

27. **Ring P., Schuck P.** The nuclear many-body problem. Berlin: Springer, 1980.

28. **Dobaczewski J., Flocard H., Treiner J.** Hartree–Fock–Bogolyubov description of nuclei near the neutron-drip line // Nucl. Phys. A. 1984. Vol. 422. No. 1. Pp. 103–139.

29. **Geng L.S., Toki H., Sugimoto S., Meng J.**

Relativistic mean field theory for deformed nuclei with the pairing correlations // Prog. Theor. Phys. 2003. Vol. 110. No. 5. Pp. 921–936.

30. **Zhou S.G., Meng J., Ring P., Zhao E.G.** Neutron halo in deformed nuclei // Phys. Rev. C. 2010. Vol. 82. No. 1. P. 011301(R).

31. **Lu B.N., Zhao J., Zhao E.G., Zhou S.G.** Multidimensionally-constrained relativistic mean-field models and potential-energy surfaces of actinide nuclei // Phys. Rev. C. 2014. Vol. 89. No. 1. P. 014323.

32. **Zhou S.G.** Multidimensionally constrained covariant density functional theories nuclear shapes and potential energy surfaces // Physica Scripta. 2016. Vol. 91. No. 6. P. 063008.

33. **Grévy S., Negoita F., Stefan I.** Observation of the  $0_2^+$  state in  $^{44}\text{S}$ , Eur. Phys. J. A. 2005. Vol. 25. No. 1 Suppl. Pp. 111–113.

34. **Tostevin J.A., Brown B.A., Simpson E.C.** Two-proton removal from  $^{44}\text{S}$  and the structure of  $^{42}\text{Si}$  // Phys. Rev. C. 2013. Vol. 87. No. 2. Pp. 027601–027604.

35. **Rodriguez-Guzmán R., Egidio J.L., Robledo L.M.** Correlations beyond the mean field in magnesium isotopes: angular momentum projection and configuration mixing // Nucl. Phys. A. 2002. Vol. 709. No. 1–4. Pp. 201–235.

36. **Raman S., Nestor C.W., Tikkanen P.** Transition probability from the ground to the first excited  $2^+$  state of even-even nuclides // Atomic Data and Nuclear Data Tables. 2001. Vol. 78. No. 1. Pp. 1–128.

37. **Möller P., Sierk A.J., Ichikawa T., Sagawa H.** Nuclear ground-state masses and deformations: FRDM (2012) // Atomic Data and Nuclear Data Tables. 2016. Vol. 109–110. Pp. 1–204.

38. **Goriely S., Chamel N., Pearson J.M.** Skyrme–Hartree–Fock–Bogolyubov nuclear mass formulas: crossing the 0.6 MeV accuracy threshold with microscopically deduced pairing // Phys. Rev. Lett. 2009. Vol. 102. No. 15. P. 152503.

Статья поступила в редакцию 29.08.2016, принята к публикации 09.10.2017.

#### СВЕДЕНИЯ ОБ АВТОРАХ

**САКСЕНА Гаурав** — сотрудник кафедры физики Правительственного женского инженерного колледжа, г. Аджмер, Индия.

Makhapura, Nasirabad Road, Ajmer, Rajasthan 305002, India  
gauravphy@gmail.com

**КАУШИК Маниш** — сотрудник кафедры физики Технологического института Шанкары, г. Джайпур, Индия.

RIICO Industrial Area (Delhi Jaipur Highway) Kukas, Jaipur, Rajasthan 302028, India  
mkaushik007@gmail.com